UNIVERSITY OF LEEDS

This is a repository copy of *Raman spectroscopy of endoscopic colonic biopsies from patients with ulcerative colitis to identify mucosal inflammation and healing*.

Raman spectroscopy of endoscopic colonic biopsies from patients with ulcerative colitis to identify mucosal inflammation and healing

James Addis,[1,*] Noor Mohammed,[2] Olorunda Rotimi,[3] Derek Magee,[4] Animesh Jha,[1] and Venkataraman Subramanian [2]

[1]*Institute of Materials Research, University of Leeds, Leeds LS2 9JT, UK*
[2]*Molecular Gastroenterology, St James University Hospital, University of Leeds, UK*
[3]*Department of Histopathology, St James University Hospital, University of Leeds, UK*
[4]*School of Computing, Faculty of Engineering, University of Leeds, UK*
[*]*j.g.addis@leeds.ac.uk*

Abstract: Raman spectroscopy was used to differentiate between mucosally healed (or quiescent) and inflamed colon tissue, as assessed endoscopically, in patients with ulcerative colitis. From the analysis of the Raman spectra of 60 biopsy tissue samples, clear differences were identified between the spectra of the quiescent and inflamed tissue. Three carotenoid peaks were found to be approximately twice as intense in the inflamed tissue. Two phospholipid peaks were found to be significantly lower in the inflamed tissue. Using multivariate statistical analysis, we show that these five peaks can be used to discriminate between endoscopically quiescent and inflamed tissue. We also correlated the Raman data with a histological assessment of the tissue. Four of the five peaks were found to be significantly different between the spectra of histologically healed (or quiescent) and histologically inflamed tissue. These findings indicate the ability of Raman spectroscopy to accurately classify colon tissue as either quiescent or inflamed, irrespective of whether an endoscopic or histological grading scheme is followed. We thus demonstrate that Raman spectroscopy could potentially be used as an early diagnosis tool for assessing the presence of mucosal healing or inflammation in patients with ulcerative colitis.

OCIS codes: (170.5660) Raman spectroscopy; (170.4580) Optical diagnostics for medicine.

References and links

1. N. A. Molodecky, I. S. Soon, D. M. Rabi, W. A. Ghali, M. Ferris, G. Chernoff, E. I. Benchimol, R. Panaccione, S. Ghosh, H. W. Barkema, and G. G. Kaplan, "Increasing Incidence and Prevalence of the Inflammatory Bowel Diseases With Time, Based on Systematic Review," Gastroenterology **142**(1), 46–54 (2012).
2. E. Langholz, P. Munkholm, M. Davidsen, and V. Binder, "Course of ulcerative colitis: analysis of changes in disease activity over years," Gastroenterology **107**(1), 3–11 (1994).
3. L. C. Dinesen, A. J. Walsh, M. N. Protic, G. Heap, F. Cummings, B. F. Warren, B. George, N. J. M. Mortensen, and S. P. L. Travis, "The pattern and outcome of acute severe colitis," J. Crohn's Colitis **4**(4), 431–437 (2010).
4. G. D'Haens, W. J. Sandborn, B. G. Feagan, K. Geboes, S. B. Hanauer, E. J. Irvine, M. Lémann, P. Marteau, P. Rutgeerts, J. Schölmerich, and L. R. Sutherland, "A review of activity indices and efficacy end points for clinical trials of medical therapy in adults with ulcerative colitis," Gastroenterology **132**(2), 763–786 (2007).
5. L. A. Feagins, S. D. Melton, R. Iqbal, K. B. Dunbar, and S. J. Spechler, "Clinical implications of histologic abnormalities in colonic biopsy specimens from patients with ulcerative colitis in clinical remission," Inflamm. Bowel Dis. **19**(7), 1477–1482 (2013).
6. J. F. Colombel, P. Rutgeerts, W. Reinisch, D. Esser, Y. Wang, Y. Lang, C. W. Marano, R. Strauss, B. J. Oddens, B. G. Feagan, S. B. Hanauer, G. R. Lichtenstein, D. Present, B. E. Sands, and W. J. Sandborn, "Early mucosal healing with infliximab is associated with improved long-term clinical outcomes in ulcerative colitis," Gastroenterology **141**(4), 1194–1201 (2011).

7. G. Pineton de Chambrun, L. Peyrin-Biroulet, M. Lémann, and J. F. Colombel, "Clinical implications of mucosal healing for the management of IBD," Nat. Rev. Gastroenterol. Hepatol. **7**(1), 15–29 (2010).
8. K. F. Frøslie, J. Jahnsen, B. A. Moum, and M. H. Vatn; IBSEN Group, "Mucosal healing in inflammatory bowel disease: results from a Norwegian population-based cohort," Gastroenterology **133**(2), 412–422 (2007).
9. M. Rutter, B. Saunders, K. Wilkinson, S. Rumbles, G. Schofield, M. Kamm, C. Williams, A. Price, I. Talbot, and A. Forbes, "Severity of inflammation is a risk factor for colorectal neoplasia in ulcerative colitis," Gastroenterology **126**(2), 451–459 (2004).
10. M. Dave and E. V. Loftus, Jr., "Mucosal healing in inflammatory bowel disease-a true paradigm of success?" Gastroenterol. Hepatol. (N. Y.) **8**(1), 29–38 (2012).
11. J. Powell-Tuck, D. W. Day, N. A. Buckell, J. Wadsworth, and J. E. Lennard-Jones, "Correlations between defined sigmoidoscopic appearances and other measures of disease activity in ulcerative colitis," Dig. Dis. Sci. **27**(6), 533–537 (1982).
12. S. A. Riley, V. Mani, M. J. Goodman, and S. Lucas, "Why do patients with ulcerative colitis relapse?" Gut **31**(2), 179–183 (1990).
13. L. Rosenberg, K. S. Nanda, T. Zenlea, A. Gifford, G. O. Lawlor, K. R. Falchuk, J. L. Wolf, A. S. Cheifetz, J. D. Goldsmith, and A. C. Moss, "Histologic markers of inflammation in patients with ulcerative colitis in clinical remission," Clin. Gastroenterol. Hepatol. **11**, 991–996 (2013).
14. S. A. Riley, V. Mani, M. J. Goodman, S. Dutt, and M. E. Herd, "Microscopic activity in ulcerative colitis: what does it mean?" Gut **32**(2), 174–178 (1991).
15. A. Bitton, M. A. Peppercorn, D. A. Antonioli, J. L. Niles, S. Shah, A. Bousvaros, B. Ransil, G. Wild, A. Cohen, M. D. D. Edwardes, and A. C. Stevens, "Clinical, biological, and histologic parameters as predictors of relapse in ulcerative colitis," Gastroenterology **120**(1), 13–20 (2001).
16. A. C. Ferrari and J. Robertson, "Resonant Raman spectroscopy of disordered, amorphous, and diamondlike carbon," Phys. Rev. B **64**(7), 075414 (2001).
17. O. J. Old, L. M. Fullwood, R. Scott, G. R. Lloyd, L. M. Almond, N. A. Shepherd, N. Stone, H. Barr, and C. Kendall, "Vibrational spectroscopy for cancer diagnostics," Anal Methods-Uk **6**(12), 3901–3917 (2014).
18. B. Mayinger, P. Horner, M. Jordan, C. Gerlach, T. Horbach, W. Hohenberger, and E. G. Hahn, "Endoscopic fluorescence spectroscopy in the upper GI tract for the detection of GI cancer: initial experience," Am. J. Gastroenterol. **96**(9), 2616–2621 (2001).
19. J. Hung, S. Lam, J. C. LeRiche, and B. Palcic, "Autofluorescence of normal and malignant bronchial tissue," Lasers Surg. Med. **11**(2), 99–105 (1991).
20. A. C. S. Talari, Z. Movasaghi, S. Rehman, and I. U. Rehman, "Raman Spectroscopy of Biological Tissues," Appl. Spectrosc. Rev. **50**(1), 46–111 (2015).
21. A. Synytsya, M. Judexova, D. Hoskovec, M. Miskovicova, and L. Petruzelka, "Raman spectroscopy at different excitation wavelengths (1064, 785 and 532 nm) as a tool for diagnosis of colon cancer," J. Raman Spectrosc. **45**(10), 903–911 (2014).
22. H. Abramczyk, B. Brozek-Pluska, J. Surmacki, J. Jablonska, and R. Kordek, "The label-free Raman imaging of human breast cancer," J. Mol. Liq. **164**(1-2), 123–131 (2011).
23. J. J. Wood, C. Kendall, J. Hutchings, G. R. Lloyd, N. Stone, N. Shepherd, J. Day, and T. A. Cook, "Evaluation of a confocal Raman probe for pathological diagnosis during colonoscopy," Colorectal Dis. **16**(9), 732–738 (2014).
24. A. Molckovsky, L. M. W. K. Song, M. G. Shim, N. E. Marcon, and B. C. Wilson, "Diagnostic potential of near-infrared Raman spectroscopy in the colon: differentiating adenomatous from hyperplastic polyps," Gastrointest. Endosc. **57**(3), 396–402 (2003).
25. P. C. Ashok, B. B. Praveen, N. Bellini, A. Riches, K. Dholakia, and C. S. Herrington, "Multi-modal approach using Raman spectroscopy and optical coherence tomography for the discrimination of colonic adenocarcinoma from normal colon," Biomed. Opt. Express **4**(10), 2179–2186 (2013).
26. X. Li, Q. B. Li, G. J. Zhang, Y. Z. Xu, X. J. Sun, J. S. Shi, Y. F. Zhang, and J. G. Wu, "Identification of Colitis and Cancer in Colon Biopsies by Fourier Transform Infrared Spectroscopy and Chemometrics," Sci World J (2012).
27. Q. B. Li, Z. Xu, N. W. Zhang, L. Zhang, F. Wang, L. M. Yang, J. S. Wang, S. Zhou, Y. F. Zhang, X. S. Zhou, J. S. Shi, and J. G. Wu, "In vivo and in situ detection of colorectal cancer using Fourier transform infrared spectroscopy," World J. Gastroenterol. **11**(3), 327–330 (2005).
28. X. Bi, A. Walsh, A. Mahadevan-Jansen, and A. Herline, "Development of spectral markers for the discrimination of ulcerative colitis and Crohn's disease using Raman spectroscopy," Dis. Colon Rectum **54**(1), 48–53 (2011).
29. C. Bielecki, T. W. Bocklitz, M. Schmitt, C. Krafft, C. Marquardt, A. Gharbi, T. Knösel, A. Stallmach, and J. Popp, "Classification of inflammatory bowel diseases by means of Raman spectroscopic imaging of epithelium cells," J. Biomed. Opt. **17**(7), 076030 (2012).
30. M. H. Mosli, B. G. Feagan, G. Zou, W. J. Sandborn, G. D'Haens, R. Khanna, C. Behling, K. Kaplan, D. K. Driman, L. M. Shackelton, K. A. Baker, J. K. MacDonald, M. K. Vandervoort, M. A. Samaan, K. Geboes, M. A. Valasek, R. Pai, C. Langner, R. Riddell, N. Harpaz, M. Sewitch, M. Peterson, L. W. Stitt, and B. G. Levesque, "Reproducibility of histological assessments of disease activity in UC," Gut **64**(11), 1765–1773 (2015).

31. T. Zenlea, E. U. Yee, L. Rosenberg, M. Boyle, K. S. Nanda, J. L. Wolf, K. R. Falchuk, A. S. Cheifetz, J. D. Goldsmith, and A. C. Moss, "Histology Grade Is Independently Associated With Relapse Risk in Patients With Ulcerative Colitis in Clinical Remission: A Prospective Study," Am. J. Gastroenterol. (2016).

32. T. Bessissow, B. Lemmens, M. Ferrante, R. Bisschops, K. Van Steen, K. Geboes, G. Van Assche, S. Vermeire, P. Rutgeerts, and G. De Hertogh, "Prognostic value of serologic and histologic markers on clinical relapse in ulcerative colitis patients with mucosal healing," Am. J. Gastroenterol. **107**(11), 1684–1692 (2012).

33. H. Abramczyk, B. Brozek-Pluska, J. Surmacki, J. Jablonska-Gajewicz, and R. Kordek, "Raman 'optical biopsy' of human breast cancer," Prog. Biophys. Mol. Biol. **108**(1-2), 74–81 (2012).

34. Q. Matthews, A. Jirasek, J. Lum, X. Duan, and A. G. Brolo, "Variability in Raman Spectra of Single Human Tumor Cells Cultured in Vitro: Correlation with Cell Cycle and Culture Confluency," Appl. Spectrosc. **64**(8), 871–887 (2010).

35. J. Surmacki, B. Brozek-Pluska, R. Kordek, and H. Abramczyk, "The lipid-reactive oxygen species phenotype of breast cancer. Raman spectroscopy and mapping, PCA and PLSDA for invasive ductal carcinoma and invasive lobular carcinoma. Molecular tumorigenic mechanisms beyond Warburg effect," Analyst (Lond.) **140**(7), 2121–2133 (2015).

36. A. Rygula, K. Majzner, K. M. Marzec, A. Kaczor, M. Pilarczyk, and M. Baranska, "Raman spectroscopy of proteins: a review," J. Raman Spectrosc. **44**(8), 1061–1076 (2013).

37. Z. Huang, A. McWilliams, H. Lui, D. I. McLean, S. Lam, and H. Zeng, "Near-infrared Raman spectroscopy for optical diagnosis of lung cancer," Int. J. Cancer **107**(6), 1047–1052 (2003).

38. J. Zhao, H. Lui, D. I. McLean, and H. Zeng, "Automated Autofluorescence Background Subtraction Algorithm for Biomedical Raman Spectroscopy," Appl. Spectrosc. **61**(11), 1225–1232 (2007).

39. K. M. Omberg, J. C. Osborn, S. L. L. Zhang, J. P. Freyer, J. R. Mourant, and J. R. Schoonover, "Raman spectroscopy and factor analysis of tumorigenic and non-tumorigenic cells," Appl. Spectrosc. **56**(7), 813–819 (2002).

40. M. G. Shim and B. C. Wilson, "The effects of ex vivo handling procedures on the near-infrared Raman spectra of normal mammalian tissues," Photochem. Photobiol. **63**(5), 662–671 (1996).

41. J. De Gelder, K. De Gussem, P. Vandenabeele, and L. Moens, "Reference database of Raman spectra of biological molecules," J. Raman Spectrosc. **38**(9), 1133–1147 (2007).

42. N. Stone, C. Kendall, J. Smith, P. Crow, and H. Barr, "Raman spectroscopy for identification of epithelial cancers," Faraday Discuss. **126**, 141–157, discussion 169–183 (2004).

43. C. Krafft, T. Knetschke, A. Siegner, R. H. W. Funk, and R. Salzer, "Mapping of single cells by near infrared Raman microspectroscopy," Vib. Spectrosc. **32**(1), 75–83 (2003).

44. I. Notingher, S. Verrier, S. Haque, J. M. Polak, and L. L. Hench, "Spectroscopic study of human lung epithelial cells (A549) in culture: living cells versus dead cells," Biopolymers **72**(4), 230–240 (2003).

45. C. Krafft, L. Neudert, T. Simat, and R. Salzer, "Near infrared Raman spectra of human brain lipids," Spectrochim. Acta A Mol. Biomol. Spectrosc. **61**(7), 1529–1535 (2005).

46. C. Krafft, T. Knetschke, R. H. W. Funk, and R. Salzer, "Identification of organelles and vesicles in single cells by Raman microspectroscopic mapping," Vib. Spectrosc. **38**(1-2), 85–93 (2005).

47. W. L. Lo, J. Y. Lai, S. E. Feinberg, K. Izumi, S. Y. Kao, C. S. Chang, A. Lin, and H. K. Chiang, "Raman spectroscopy monitoring of the cellular activities of a tissue-engineered ex vivo produced oral mucosal equivalent," J. Raman Spectrosc. **42**(2), 174–178 (2011).

48. R. Tuma, "Raman spectroscopy of proteins: from peptides to large assemblies," J. Raman Spectrosc. **36**(4), 307–319 (2005).

49. J. W. Chan, D. S. Taylor, T. Zwerdling, S. M. Lane, K. Ihara, and T. Huser, "Micro-Raman spectroscopy detects individual neoplastic and normal hematopoietic cells," Biophys. J. **90**(2), 648–656 (2006).

50. C. J. Frank, R. L. McCreery, and D. C. B. Redd, "Raman spectroscopy of normal and diseased human breast tissues," Anal. Chem. **67**(5), 777–783 (1995).

51. I. V. Ermakov, M. Sharifzadeh, M. Ermakova, and W. Gellermann, "Resonance Raman detection of carotenoid antioxidants in living human tissue," J. Biomed. Opt. **10**(6), 064028 (2005).

52. N. Uzunbajakava, A. Lenferink, Y. Kraan, B. Willekens, G. Vrensen, J. Greve, and C. Otto, "Nonresonant Raman imaging of protein distribution in single human cells," Biopolymers **72**(1), 1–9 (2003).

53. J. C. Merlin, "Resonance Raman-Spectroscopy of Carotenoids and Carotenoid-Containing Systems," Pure Appl. Chem. **57**(5), 785–792 (1985).

54. H. Abramczyk, M. Kolodziejski, and G. Waliszewska, "Vibrational relaxation of beta-carotene in acetonitrile solution in carrot in situ," J. Mol. Liq. **79**(3), 223–233 (1999).

55. W. T. Cheng, M. T. Liu, H. N. Liu, and S. Y. Lin, "Micro-Raman spectroscopy used to identify and grade human skin pilomatrixoma," Microsc. Res. Tech. **68**(2), 75–79 (2005).

56. C. H. Chuang and Y. T. Chen, "Raman scattering of L-tryptophan enhanced by surface plasmon of silver nanoparticles: vibrational assignment and structural determination," J. Raman Spectrosc. **40**(2), 150–156 (2009).

57. T. G. Spiro and T. C. Strekas, "Resonance Raman Spectra Of Heme Proteins. Effects of Oxidation and Spin State," J. Am. Chem. Soc. **96**(2), 338–345 (1974).

58. H. Brunner, H. Sussner, and A. Mayer, "Resonance Raman Scattering on Heme Group of Oxyhemoglobin Deoxyhemoglobin," J Mol Biol **70**, 153–156 (1972).

59. S. K. Bai, S. J. Lee, H. J. Na, K. S. Ha, J. A. Han, H. Lee, Y. G. Kwon, C. K. Chung, and Y. M. Kim, "beta-Carotene inhibits inflammatory gene expression in lipopolysaccharide-stimulated macrophages by suppressing redox-based NF-kappaB activation," Exp. Mol. Med. **37**(4), 323–334 (2005).

1. Introduction

Ulcerative colitis (UC) is a chronic inflammatory condition, which is diagnosed in patients worldwide, irrespective of ethnicity and anthropological origin, and is becoming more prevalent with time. Amongst the human population, UC has a current annual incidence of 24.3 per 100,000 person-years in Europe, 6.3 per 100,000 person-years in Asia and the Middle East, and 19.2 per 100,000 person-years in North America [1]. UC is of unknown aetiology, characterised by diffuse and confluent mucosal inflammation of the colon, starting from the rectum with a characteristic relapsing and remitting course [2]. Approximately 25% of patients with UC experience acute exacerbation of their disease activity during the course of their disease [3]. The colectomy rate increases with more than one hospital admission with acute severe UC reaching up to 40% after two admissions [3]. Therefore, the treatment goals in UC focus on keeping the disease in remission and a colectomy free survival. A critical part of the assessment of UC is the definition of what constitutes clinical remission.

To that end, the notion of mucosal healing (MH) has become increasingly important as a measure of the activity of the disease. The International Organisation of Inflammatory Bowel Disease (IBD) has proposed the following criteria to define MH: the absence of friability, blood, erosions and ulcers in all visualised segments of the gut mucosa [4]. (However, it should be noted that there is no consensus definition). In essence, MH is characterised by the disappearance of endoscopic lesions such as erosions and ulcers. If MH is achieved then the short and long term clinical outcomes for the patient tend to be favourable. For example, reduced hospitalisation due to flares, decreased colectomy rates and lower incidence of colorectal cancers are all associated with MH [5–9]. MH is thus becoming recognised as a desirable therapeutic endpoint not only in clinical trials but also in routine clinical practice.

Two of the common, clinical techniques used for the diagnosis and assessment of UC are endoscopy and histopathology. The presence or absence of MH in patients diagnosed with UC is usually assessed by endoscopy [10]. Conventional endoscopy was thought to be a reliable parameter for the assessment of the disease activity in UC [11]. However, it is recognised that microscopic inflammation can persist despite normal mucosal findings [12]. Examination for MH can also be done by histopathology [13]. This technique is useful, as histologically detectable inflammation has been shown to be associated with a greater risk of subsequent relapse [14, 15]. That said, irrespective of whichever technique is used, a flare in UC activity remains difficult to predict. Therefore, a simple, easily measured biological marker that predicts relapse would be of great use in guiding the most appropriate and cost-effective therapy. Developing a complementary tool that can reliably and quickly identify the presence of inflammation or confirm that MH has occurred would help to guide patient management.

In this respect, molecular vibrational spectroscopic analysis is a strong candidate for such a tool. Molecular vibrational spectroscopic analysis is used to characterise solids, liquids and gases and is especially relevant when the analyte is rare to procure and small in size for analysis, as is the case for endoscopic biopsy specimens of typical surface area ~5 mm^2. Further, vibrational spectroscopy has huge potential in medicinal applications as it is non-destructive and has the ability to reveal the biochemistry of tissue. This allows, in principle, differentiation between healthy and anomalous tissue.

Raman spectroscopy was chosen as the vibrational spectroscopic technique for this study. In a Raman microscope, as used in this study, incident monochromatic light of modest power (< 10 mW), controlled by focussing through an objective lens, is directed at the sample. The light scattered by the sample is collected and detected. Raman scattering is an inelastic scattering process for which the probability of occurrence is 1000-100,000 times less than that

of Rayleigh scattering. Only molecular vibrations which involve changes in the polarisability of the molecule are Raman active. In this respect, the vast majority of biomolecules provide rich Raman spectra as they have complex ring-like aromatic and/or long-chain aliphatic structures, which may be interconnected to enhance the probability of inelastic scattering, and, as a result, may be more Raman active. Such extended local order in the structures of biomolecules limits the dispersion of energy states in the resulting Raman spectra. Consequently, the peaks have well defined shapes, unlike in amorphous materials where the lack of medium and long-range order yields dispersed phonon energy states [16]. In analytes consisting of multiple constituent molecules, a spectrum of Raman scattered light consists of a range of peaks corresponding to the Raman active-vibrational modes, stimulated by the incident laser. The peak intensities are proportional to the concentrations of the responsible molecules. The resultant spectrum may therefore be interpreted as a qualitative and quantitative measure of the analyte biochemistry [17]. Importantly, the OH vibrational modes of water molecules produce weak Raman signals and thus do not contribute significantly to Raman spectra. This is in contrast to infrared (IR) spectroscopy where OH- ions and free water, often present in biomolecular and tissue media, are highly absorptive in the mid IR range from 2.7 to 4.5 μm. The absorption peaks of water thus tend to overlap with those due to representative aromatic ring C-C (wavenumber 1600-1585 cm^{-1}, 1500-1400 cm^{-1}), hydrocarbon C-H (2850-3100 cm^{-1}) and C = O (1630-1780 cm^{-1}) stretch vibrations of biomolecules. Fluorescence spectroscopy can also be used to characterise tissue. Once again in complex molecules a range of electron-phonon coupled states might arise during excitation which during fluorescence decay might yield a broad spectrum of spontaneous emission. Fluorescence spectra from tissue thus tend to be relatively broad and featureless [18] with fewer specific differences in the spectra from healthy and anomalous tissue [19]. In comparison, Raman spectroscopy has the advantage of delivering spectra with sharp, narrow peaks in different parts of the spectrum for lipids, proteins and nucleic acids [20]. The main disadvantages of Raman spectroscopy are that the scattered intensity is inherently weak and that the Raman excitation laser can induce the aforementioned fluorescence in tissue, which can obscure the weak Raman signal [21]. Despite these drawbacks, Raman spectroscopy has been shown to be successful in providing very sensitive biochemical information about the composition of biological tissue [22].

A number of vibrational spectroscopy studies have been performed on human colon tissue. Most of these studies have attempted to use vibrational spectroscopy to distinguish either between colon tissue containing polyps and healthy tissue or between cancerous and healthy tissue [23–27]. However, very few studies have employed spectroscopy to study UC. Two such studies on UC and Crohn's disease [28, 29] examined respectively, 21 and 38 samples.

In this study, therefore, we perform Raman spectroscopy on a large sample set (60 samples) of colonic biopsies, taken from patients who have been diagnosed with UC and are either in remission or still have the condition. We analyse the ability of Raman spectroscopy to differentiate between tissue that has, from an endoscopic point of view, mucosally healed and tissue for which endoscopic inflammation is still present. We provide insights into the pathogenesis of UC and put forward a biological explanation for the differences observed in the levels of certain biomolecules between quiescent and inflamed tissue. In addition, we assess a second set of colonic biopsies, taken from the same patients at the same sites at the same time as the first set, for histological activity. We assess whether Raman spectroscopy also provides a reliable means of discriminating between tissue that has, from a histological point of view, healed and tissue for which histological inflammation is still observable. We thus evaluate the ability of Raman spectroscopy to distinguish between quiescent and inflamed tissue, which has been graded by two different clinical techniques; endoscopy and histopathology. In this way, we aim to provide a more complete assessment of the utility of Raman spectroscopy as a potential, complementary tool for the assessment of UC.

2. Experiment

2.1 Patients, samples and tissue preparation

All patients in the study had initially been diagnosed with UC at the IBD clinic at St James University hospital, Leeds, had followed a course of treatment and returned to the IBD clinic for further assessment during colonoscopy. Informed consent was obtained from all patients and ethical approval for the study including the collection of biopsies for spectroscopy and histological assessment was obtained from the Yorkshire and Humber–Yorkshire Bridge National Research Ethics Committee (13YH-0115).

During colonoscopy the colonic tissue was assessed endoscopically for endoscopic MH by expert (gastrointestinal GI) endoscopists, using the Mayo endoscopic score (See Table 1) [34], and a score was assigned. A score of zero was taken to indicate that endoscopic MH had occurred and all scores greater than 0 indicated that endoscopic inflammation was still present (i.e. an absence of endoscopic MH).

Table 1. Mayo endoscopic score

Score	Description
0	Normal / inactive disease
1	Mild disease (Erythema, decreased vascular pattern, mild friability)
2	Moderate disease (Marked erythema, absent vascular pattern, friability, erosions)
3	Severe disease (Spontaneous bleeding, ulceration)

Biopsies for the purposes of the Raman spectroscopy study and the histological assessment were then taken from the same area assessed by endoscopy. The sample dimensions of surgically removed biopsies were typically of length ~3 to 4 mm, width ~1.5 to 2 mm and thickness ~1 to 2 mm. For both the Raman study and the histological assessment, 60 biopsies were collected from 39 patients; 32 from the sigmoid and 28 from the rectum. Of the 60 samples for the Raman study, 24 were taken from areas with endoscopic MH and 36 from areas with signs of endoscopic inflammation. Immediately after taking the biopsies, they were snap-frozen in liquid nitrogen and stored at −80°C. The prompt snap-freezing of biopsies allowed the metabolic content of the tissue to be preserved as in the in-vivo state, as required to obtain Raman spectra which accurately reflect their biochemical composition at the time of collection of the biopsies. 60 biopsies were also taken at the same sites at the same time for the histological assessment. These were fixed in formaldehyde and then later stained with haematoxylin and eosin. These were graded histopathologically by an expert GI histopathologist (O.R.), using the validated Geboes scoring system, which has been shown to have the best inter-observer agreement [30]. A Geboes score of less than 3.1 was considered to indicate that the mucosa had histologically healed and a score of 3.1 or greater to denote histological activity (HA), when there is the presence of neutrophils in the epithelium [31, 32]. Of these 60 samples, 27 were graded as histologically healed and 33 as histologically active (HA). In both the endoscopically assessed and in the histologically assessed groups of samples we can thus consider that there is a population of tissue samples with the status quiescent and another population with the status inflamed.

We compared the status given to each sample during endoscopic assessment with that given during histological assessment. Disagreement between the endoscopic and histological assessments of the tissue status was observed in 5 samples out of 60. The assessments of the tissue status via the two techniques, as being either quiescent or inflamed, thus matched for 92% of the samples, as might be expected for two techniques that are complementary.

2.2 Raman spectroscopy

We used an inVia Renishaw Raman microscope to obtain the Raman spectra for the tissue samples. Samples were removed from the −80°C freezer and placed on to low fluorescence glass microscope slides on the microscope stage. Samples were not rehydrated in saline. A

continuous wave (cw) laser of wavelength 514.5 nm and 5 mW incident power was used as the excitation source. The laser beam was focused by a 50x microscope objective of numerical aperture 0.8 and working distance 1.1 mm to form a spot of diameter ~5 μm on the sample surface. Single scan exposures of 10 seconds were sufficient to obtain a good signal-to-noise ratio. The values used for the incident laser power, spot size and exposure time lead to an energy density which is similar or slightly lower than that employed in other Raman spectroscopy studies on tissue [25, 33, 34]. The constituency, shape and composition of a biopsy sample can vary significantly from one region to another on its surface. Hence spectra were taken at four different points per sample. Spectra were collected for the Raman shift range of 400 to 3000 cm^{-1} with a spectral resolution of 4 cm^{-1}. This range and resolution are relatively favourable with respect to typical Raman instruments, which often provide a range of 700 to 1800 cm^{-1} and a resolution of 6 to 8 cm^{-1}, and are similar to those used in some recent Raman studies on colon tissue [35, 36].

2.3 Processing of Raman spectra

For each sample the average Raman spectrum was calculated from the four measurements taken. As mentioned in Section 1, tissue may produce fluorescence when excited with a short wavelength visible laser for Raman spectroscopy. The measured spectrum thus consists of Raman scattered light, fluorescent light emitted by the tissue (the fluorescent background) and noise [37]. Three operations were performed; i) data smoothing, ii) background estimation and subtraction and iii) normalisation of the background-corrected spectrum. Data smoothing was achieved using a Savitzky-Golay filter with a smoothing width of 9 and polynomial of degree 3 in order to increase the signal-to-noise ratio [25]. An effective method for estimating the fluorescence background is modified polynomial fitting [38] and this technique was found to be optimal for the spectra in this study. The adapted polynomial form was subtracted from the averaged, smoothed spectrum to obtain the uncluttered Raman spectrum consisting of a set of peaks with a relatively flat baseline. In a Raman microscope, the cone of light backscattered from the sample, which enters the objective, forms the signal measured. For a particular illuminated sample area, the signal measured therefore depends not only on the concentrations of the Raman-active molecules in the area but also on the shape and the reflectivity of the surface and the accuracy of focussing on the surface. Since the biopsies were non-uniform and uneven, these factors lead to large variations in the signal measured from area to area on the sample and from sample to sample. To correct for the variations in absolute signal intensity and thus to be able to compare the peak intensities between samples, each background-corrected spectrum was thus normalised by dividing by the total area under the curve [34].

2.4 Statistical methods

For the evaluation of diagnostic sensitivity and tissue classification, two-tailed non-parametric Mann-Whitney U tests to identify statistically significant differences between the peak intensities in the Raman spectra for different sample groups were performed. One test was carried out on the Raman data for the group of samples assessed endoscopically in order to highlight the differences between the spectra of samples taken from areas of the colon which showed endoscopic MH and of those taken from areas which showed endoscopic inflammation. A second such test was performed on the group of samples assessed histologically in order to quantify the spectral differences between the samples which showed histological healing and those which showed HA. Non-parametric tests were used as the distribution of the Raman spectral peak intensities did not follow a normal distribution. A p value of ≤ 0.05 was used as a cut-off of significance. Results are expressed as the mean ± standard deviation for continuous variables.

Multivariate analysis was also performed by logistic regression analysis to calculate odds ratios (OR) and their 95% confidence intervals. All variables with a p value of < 0.1 in the

Mann-Whitney U analysis were included (as planned a-priori) in the final multivariate model. Correlation matrices were used to identify collinearity. If collinearity was detected we minimised this by inputting the variable separately in the multivariate analysis. Hosmer-Lemeshow's test was used to verify the null hypothesis that there is a linear relationship between the predictor variable and the log odds of the outcome variable. All statistical tests were done using PASW version 21 (IBM Corp, NY).

3. Results and discussion

3.1 Analysis of Raman spectra

Figure 1 displays the average Raman spectra of the endoscopically assessed biopsy samples taken from areas of the colon which showed endoscopic MH and of those taken from areas which showed endoscopic inflammation (i.e. where endoscopic MH was absent).
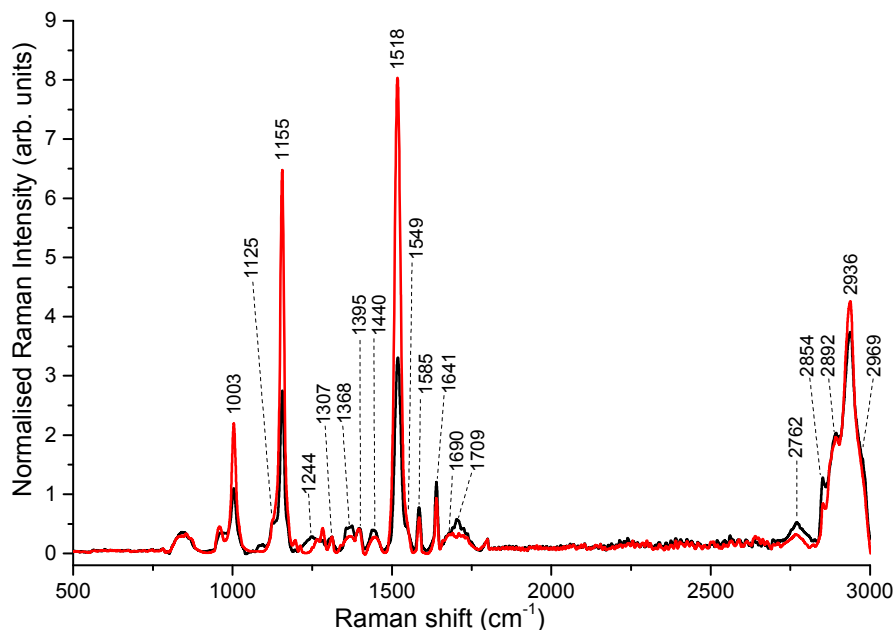

Fig. 1. Average background-subtracted normalised Raman spectra for endoscopically assessed colonic mucosa which showed either a) endoscopic MH (black) or b) endoscopic inflammation (red).

The form of the spectra for both the colonic mucosa which showed endoscopic MH and those which exhibited endoscopic inflammation is similar with primary peaks observable at Raman shifts of 1003, 1155, 1244, 1307, 1368, 1395, 1440, 1518, 1585, 1641, 1690, 1709, 2762 and 2936 cm^{-1} and shoulder peaks at 1125, 1549, 2854, 2892 and 2969 cm^{-1}. Strong peaks are found in both tissue types at 1003, 1155, 1518 (the largest peak in the endoscopically inflamed tissue), 2762, 2892 and 2936 cm^{-1} (the largest peak in the endoscopic MH tissue). The most striking difference between the two tissue types is in the intensity of the peaks at 1003, 1155 and 1518 cm^{-1}. These are considerably higher in the endoscopically inflamed than in the endoscopic MH tissue.

In terms of constituent biomolecules, both spectra contain contributions from vibrational modes of proteins, amino acids, lipids and nucleic acids as well as other compounds such as carotenoids and myoglobin. A detailed list of the peaks observed and their possible assignments is described in Table 2. Regarding the peaks at 1125, 1307, 1368 and 1395 cm^{-1}

several different assignments for each one are possible. The peak at 1125 cm^{-1} could be attributed to vibrations of phospholipids or proteins [39]; the peak at 1307 cm^{-1} could be assigned to phospholipids [39] or lipids [40] or the nucleotide, adenine [41]; the peak at 1368 cm^{-1} to the nucleotides, guanine [42] or thymine [43], or to the amino acid, tryptophan [39], and that at 1395 cm^{-1} to the nucleotide, uracil [41]. However, the fact that these four peaks as well as peaks at 1549 cm^{-1} (assigned to deoxy-myoglobin in colon tissue [21]) and at 1585 cm^{-1} and 1641 cm^{-1} (both assigned to oxy-myoglobin in colon tissue [21]) are present in the spectra plus the experimental observation that the inflamed colonic mucosa often showed signs of bleeding mean that we assign the peaks at 1125, 1307, 1368 and 1395 cm^{-1} to haeme groups, in particular to the haeme core of myoglobin [21]. In terms of the other peaks, the peak at 1440 cm^{-1} is characteristic of scissoring vibrations of CH_2 in phospholipids [37] and lipids [40]. Signals characteristic of the amide bands of proteins are found at 1244 cm^{-1} (amide III, β-sheet conformation [44]) and 1690 cm^{-1} (amide I, β-sheet conformation [34]). The band at 1709 cm^{-1} is consistent with C = O vibrations in phospholipids and triglycerides [45]. The signal at 2762 cm^{-1} corresponds to a CH stretch, possibly in phospholipids [46]. Vibrations that are characteristic of the CH groups in lipids (fatty acids, triglycerides) are observed at: 2854 cm^{-1} (symmetric stretching of the CH_2 group [43]), 2892 cm^{-1} (antisymmetric stretching of the CH_2 group [43]), 2936 cm^{-1} (symmetric stretching of the CH_3 group [33, 43]) and 2969 cm^{-1} (antisymmetric stretching of the CH_3 group [43]).

Table 2. Tentative assignments of peaks in Raman spectra of colon tissue

Peak no.	Centre (cm^{-1})	Vibrational mode	Major assignments
1	1003	Ring breathing ρ(C-CH$_3$)	Phenylalanine [47–50] Carotenoids [35,51]
2	1125	ν_{22}-ν(Pyr ½ ring)$_{as}$ ν(C–C) ν(C–N)	Myoglobin (haeme core) [21] Phospholipids [39] Proteins [39,52]
3	1155	ν(C–C)	Carotenoids [22,51,53,54]
4	1244		Amide III, β-sheet [44]
5	1307	τ(CH$_2$) ν_{21}-δ_{as}(C$_m$H)	Phospholipids [39], lipids [40] Adenine [41] Myoglobin (haeme core) [21]
6	1368	ω(CH$_2$), δ(CH) ν_4-ν(Pyr ¼ ring)$_s$	Tryptophan [55,56] Guanine [42] Thymine [43] Myoglobin (haeme core) [21]
7	1395	ν_{20}-ν(Pyr ¼ ring)	Myoglobin (haeme core) [21] Uracil [41]
8	1440	δ_{sc}(CH$_2$) δ(CH$_2$), δ(CH$_3$)	Phospholipids [37], lipids [40] Collagen [31]
9	1518	ν(C = C)	Carotenoids [22,51,53,54]
10	1549	ν_{11}-ν(C$_\alpha$C$_\beta$)$_{as}$	Deoxy-Myoglobin (haeme core) [21,57,58]
11	1585	δ(C = C) ν_{37}-ν(C$_\alpha$C$_m$)$_{as}$	Phenylalanine [37,55] Hydroxyproline [27] Oxy-Myoglobin (haeme core) [21,57,58]
12	1641	ν_{10}-ν(C$_\alpha$C$_m$)$_{as}$	Oxy-Myoglobin (haeme core) [21,57]
13	1690		Amide I, β-sheet [34]
14	1709	ν(C = O)	Phospholipids [45], triglycerides [45]
15	2762	ν(C-H)	Phospholipids [46]
16	2854	ν_s(CH$_2$)	Lipids [34,35,43]
17	2892	ν_{as}(CH$_2$)	Lipids [34,35,43], proteins [39]
18	2936	ν_s(CH$_3$)	Lipids [22,34,43], proteins [39]
19	2969	ν_{as}(CH$_3$)	Lipids [34,43], proteins [39]

ν – stretching vibration; ν_s – symmetric stretch; ν_{as} – antisymmetric stretch; δ – bending vibration; δ_{sc} – in-plane bending (scissoring); ρ – in-plane bending (rocking); τ – out-of-plane bending (twisting); ω – out-of-plane bending (wagging).

Considering the three sharp peaks at 1003, 1155 and 1518 cm^{-1}, the peak at 1003 cm^{-1} has previously been considered to be due to phenylalanine [48]. However, when peaks at 1155 cm^{-1} and 1518 cm^{-1} are also present, forming the triplet combination seen in Fig. 1, it has become common to assign these three peaks to vibrations of carotenoids [33, 35, 51]. In an attempt to improve the characterisation of the carotenoid groups, we have compared our data with the Raman data for a wide range of carotenoids. Three different characteristic vibrations are identified in [53]. The most dominant phonon vibration is the approximate in-phase stretching vibration of C = C bonds (v_1, 1490-1540 cm^{-1}), followed by the C-C stretching mode (v_2, 1140-1160 cm^{-1}), which may be mixed with C-H in-plane vibrations, and, finally, the in-plane rocking mode of CH$_3$ (v_3, ~1005 cm^{-1}). This vibration is part of the carotenoid "fingerprint region" from 1100 to 1400 cm^{-1}, which contains weak peaks sensitive to the terminal groups and chain conformation in the carotenoid. In our data the peaks at 1003 cm^{-1} (in-plane rocking of CH$_3$), 1155 cm^{-1} (stretching of C-C) and 1518 cm^{-1} (stretching of C = C) are thus consistent both in terms of position and relative intensities with the data reported for carotenoids [53].
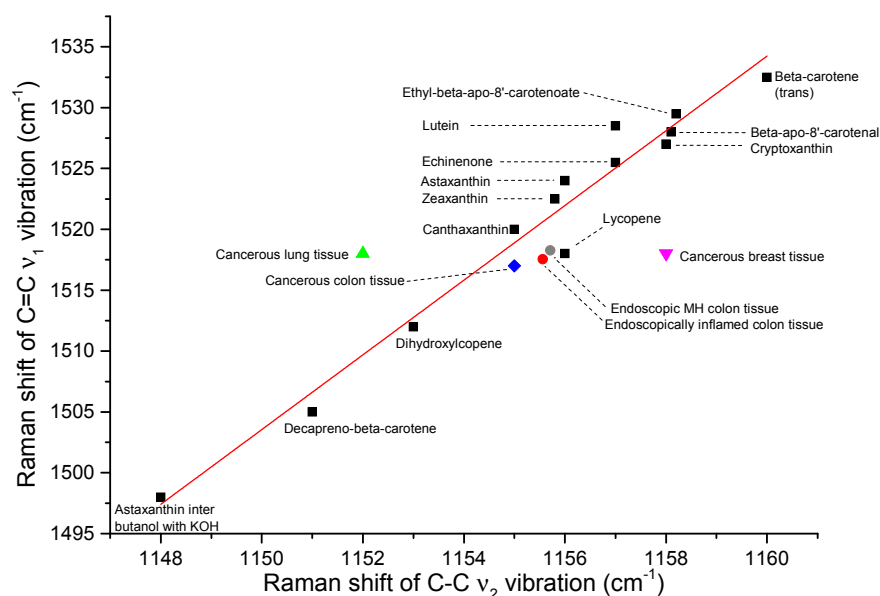

Fig. 2. Plot of frequency of C = C (v_1) versus C-C stretching vibration (v_2) for beta-carotene isomers (black squares, values from [53]), colonic mucosa showing endoscopic MH (grey circle, our data), colonic mucosa showing endoscopic inflammation (red circle, our data), cancerous colon tissue (blue diamond [21],), cancerous breast tissue (pink triangle [22],), cancerous lung tissue (green triangle [37],). Figure adapted from [53].

We take the analysis of our data further by examining the relationship between π-electron conjugation and the wavenumber of the C-C stretching mode (v_2) for different carotenoids. In polyenes, such as carotenoids, as the number of C = C double bonds and, in that way, length of the conjugated chain increases, the space for the Π electrons to delocalise increases, leading to a decrease in the order of the C = C bond. This causes a reduction in bond strength and thus a decrease in the frequency of vibration of the C = C stretching mode (v_1). This can be seen in Fig. 2., where, for example, v_1 for decapreno-beta-carotene, which has 10 more C atoms than beta-carotene, is 25 cm^{-1} lower than for beta-carotene. A decrease in the position of the v_1 mode is usually accompanied by an increase in the position of the v_2 mode [53]. However, interestingly, carotenoids show the opposite trend in Fig. 2. This may be due to the

presence of CH_3 groups which disturb the C-C stretching modes [53]. From Fig. 2 we suggest, that in both our colonic mucosa which showed endoscopic MH and in those with endoscopic inflammation, the carotenoid found may be of canthaxanthin and lycopene types. The carotenoid present in cancerous colon tissue [21] also appears to be of these types.

3.2 Statistical analysis of data

In Fig. 3 we compare the average Raman peak intensities of the endoscopically assessed biopsy samples which showed endoscopic MH with those of the samples which showed endoscopic inflammation. The p values, obtained in the non-parametric Mann Whitney U test for this group of endoscopically assessed samples, are also shown in Fig. 3.
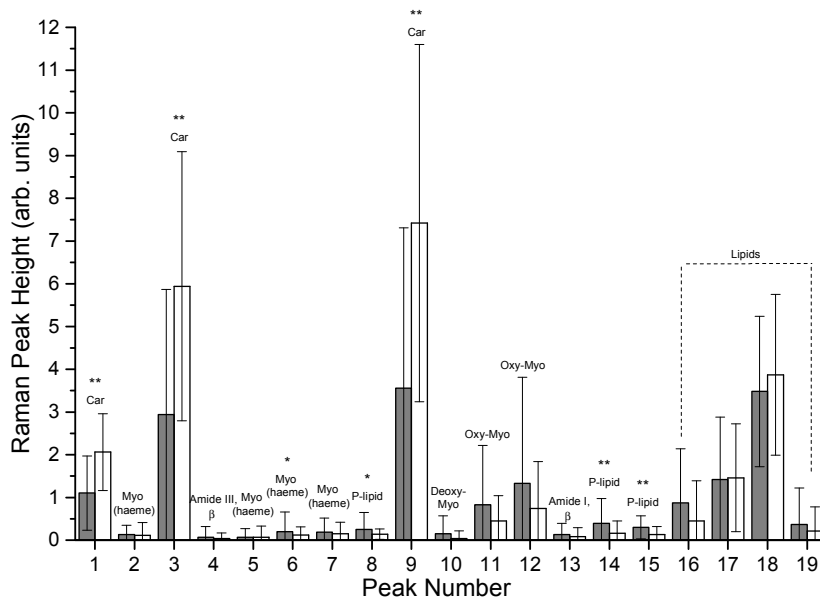

Fig. 3. Histogram displaying average Raman peak intensities, standard deviations and p values for endoscopically assessed colonic mucosa which showed either a) endoscopic MH (N = 24, filled grey) or b) endoscopic inflammation (N = 36, unfilled). No asterisk represents p > 0.10, a single asterisk * represents 0.10 ≥ p > 0.05 and two asterisks ** represent p ≤ 0.05. Abbreviations: Car = carotenoids; Myo = myoglobin, Oxy-Myo = oxy-myoglobin, Deoxy-Myo = deoxy-myoglobin, P-lipid = phospholipids.

It can be seen from Fig. 3 that in the endoscopically inflamed tissue the average intensity of the carotenoid peak at 1003 cm^{-1} is ~75% greater than in the endoscopic MH tissue, whilst the carotenoid peaks at 1155 cm^{-1} and 1518 cm^{-1} are almost double those in the endoscopic MH tissue. The standard deviation of the peak intensities is substantial, which reflects the inhomogeneity of the tissue samples. Differences in the peak intensity between endoscopic MH and endoscopically inflamed tissue with a significance level of $p \leq 0.05$ are found for peaks 1 (1003 cm^{-1}), 3 (1155 cm^{-1}), 9 (1518 cm^{-1}), 14 (1709 cm^{-1}) and 15 (2762 cm^{-1}). Differences with a significance level of $0.10 \geq p > 0.05$ are obtained for peaks 6 (1368 cm^{-1}) and 8 (1440 cm^{-1}). These statistics clearly indicate that the Raman spectral differences between endoscopic MH and endoscopically inflamed colon tissue are significant and are consistent with previous reports [28, 29].

Figure 4 presents the same information as Fig. 3 but for the group of histologically assessed samples. The p values come from the non-parametric Mann Whitney U test for this group.
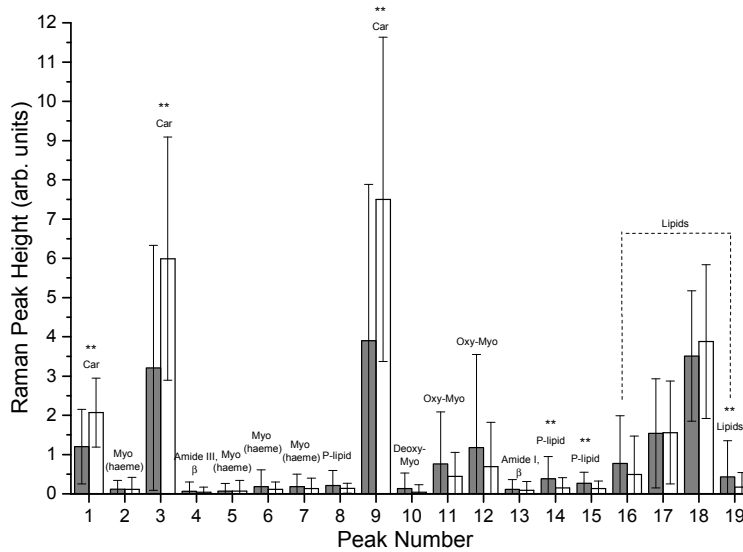
Fig. 4. Histogram displaying average Raman peak intensities, standard deviations and p values for histologically assessed colonic mucosa which showed either a) histological healing (N = 27, filled grey) or b) HA (N = 33, unfilled). The same key and abbreviations as for Fig. 3. apply.

The peak intensities are very similar to those in Fig. 3, with the carotenoid peaks much greater in the samples which showed HA than in the samples which exhibited histological healing. Differences in the peak intensity between histologically healed samples and samples which showed HA with a significance level of $p \leq 0.05$ are again observed for peaks 1, 3, 9, 14, 15 and also 19 (2968 cm^{-1}). Just as for the endoscopically assessed group, Fig. 4 indicates that there are significant differences in the Raman spectra of histologically healed and histologically active samples.

The non-parametric analysis is extended to a multivariate analysis, which has been shown to be more accurate and reliable when analysing multiple peaks over a large Raman spectral range [24], as is the case for our colon tissue spectra. The results of the multivariate analysis are presented in Table 3.

Table 3. Multivariate analysis for the a) endoscopically assessed group and b) histologically assessed group of colonic mucosa

Peak no.	a) Endoscopically assessed group Endoscopic inflammation (N = 36) versus endoscopic MH (N = 24) OR (95% CI)	b) Histologically assessed group HA (N = 33) versus histologically healed (N = 27) OR (95% CI)
1#	**3.71 (1.79-7.67)**	**1.92 (1.28-2.87)**
3#	**1.50 (1.19-1.89)**	**1.22 (1.07-1.39)**
6	0.68 (0.05-9.48)	N/A
8	**0.05 (0.004-0.55)**	N/A
9#	**1.36 (1.14-1.61)**	**1.17 (1.09-1.30)**
14	0.68 (0.15-3.04)	0.48 (0.08-2.80)
15	**0.24 (0.09-0.64)**	**0.40 (0.19-0.84)**
19	N/A	0.65 (0.21-2.04)

inputted separately into the model as they were highly correlated (rho > 0.6). Significant differences are in **bold**. N/A implies the p value of the peak in the Mann Whitney U test was > 0.10 and therefore was not included in the multivariate analysis.

In the multivariate model peaks 1, 3, 8, 9 and 15 turn out to be significantly different between endoscopic MH and endoscopically inflamed samples. All of these except peak 8 are

also significantly different between histologically healed samples and samples which showed HA.

A visual comparison is presented in the 3D scatter plots in Figs. 5(a) and 5(b) which show the distribution of the intensity of the important peaks 1, 3 and 15 in the groups assessed endoscopically and histologically. In both figures the separation between the two populations (the quiescent population and the inflamed population) is clearly visible. Both figures suggest that in a Raman spectrum where peaks 1 and 3 are high, whilst in comparison peak 15 is medium to low, the sample is more likely to be inflamed than quiescent. The strong likeness between the distributions in both figures is to be expected in view of the close match between the endoscopy and histology grades for the vast majority of samples.
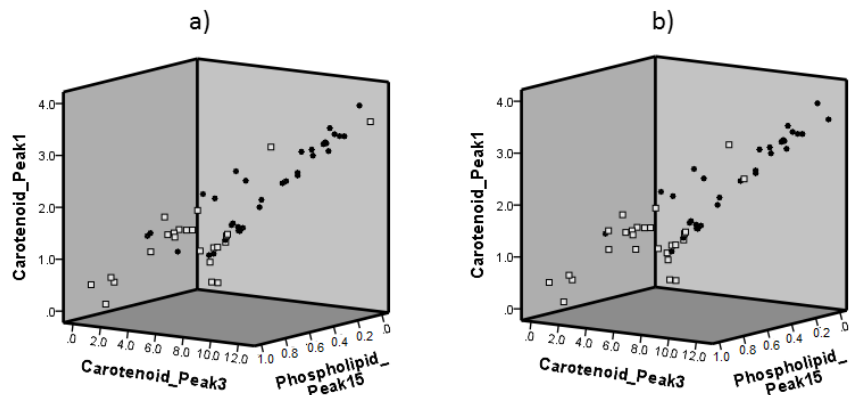

Fig. 5. Scatter plot of intensities of peaks 1, 3 and 15 for a) endoscopically assessed colonic mucosa which showed either endoscopic MH (open squares) or endoscopic inflammation (filled circles) and b) histologically assessed colonic mucosa which showed either histological healing (open squares) or HA (filled circles).

3.3 Biomolecular explanation for differences between quiescent and inflamed Raman spectra

We attempt to explain the similarities and differences between the Raman spectra of colonic mucosa showing endoscopic MH and of colonic mucosa showing endoscopic inflammation in terms of the biomolecular composition of the mucosa, based on the peak assignments made in Section 3.1. The fact that the same set of peaks occurs in both the endoscopic MH and endoscopically inflamed tissue indicates that their biochemical composition is very similar. This is consistent with common understanding of inflammation. Inflammation does not introduce new metabolites to the system but rather leads to overproduction or overuse of the existing metabolites. One would thus expect the same peaks to be found in the two tissue types. Variations in peak intensities between the two tissue types are due to differences in the concentrations of biomolecules in the two. The endoscopically inflamed tissue contains very high amounts of carotenoids. Carotenoids are known to act as anti-oxidants [22] in the defence mechanism of tissue against inflammation. Beta-carotene for instance has been shown to supress the activation of nuclear factor kappa-beta and thereby inhibit pro-inflammatory gene expression [59]. Carotenoid compounds could thus be expected to be strongly present in endoscopically inflamed tissue, as observed. Additionally, we found that the phospholipid components (peak 8 at 1440 cm^{-1} and peak 15 at 2762 cm^{-1}) were markedly higher in samples where endoscopic MH had occurred. This observation would reflect the fact that when, endoscopically, tissue is visibly inflamed, there is a marked loss of tissue integrity, characterised by ulceration or erosion of the mucosa with loss of the cell membrane. Phospholipids are well known to be a major component of the colonic cell membrane and if tissue is disrupted, as is the case when it is inflamed, their levels would be expected to decrease.

4. Conclusion

An emerging goal of gastroenterology is to establish whether mucosal healing (MH) has occurred in patients treated for UC, as MH appears to lead to favourable outcomes for the patient. To this end, a spectroscopic tool which could assist current techniques such as endoscopy and histopathology in examining colonic mucosa for evidence of MH would be of great benefit. In this study we thus employed Raman spectroscopy to evaluate its potential for such a tool.

60 biopsy samples were taken from areas of the colon which showed endoscopic MH and from areas which showed endoscopic inflammation, snap frozen at $-80°C$ in order to preserve their metabolic content and their Raman spectra were obtained. Simultaneously, we collected a second group of 60 samples from these areas of the colon and assessed them histologically.

We analysed the Raman spectra of the colonic mucosa, assigned the peaks to vibrations of biomolecules and performed Mann Whitney U analyses and multivariate statistical analyses on the spectral peak intensities. The essential findings can be summarised as follows:

1. A similar set of Raman peaks corresponding to vibrations of proteins, amino acids, lipids, nucleic acids, myoglobin and carotenoids was observed in the endoscopic MH and the endoscopically inflamed tissue, indicating that similar biomolecules are present in each. This suggests that inflammation can be thought of as a state of activity where greater or lower quantities of existing biomolecules are produced by the body's response.

2. The major visual difference between the Raman spectra of the biopsy samples which showed endoscopic MH and those which showed endoscopic inflammation was found to be in three carotenoid peaks. Carotenoid levels were found to be very high (almost double) in the inflamed compared to in the quiescent tissue. This finding is consistent with the role they play as anti-oxidants in fighting inflammation. Significant differences were also observed in two phospholipid peaks. Phospholipid levels were found to be lower in the inflamed tissue. This is also consistent with studies which indicate that phospholipids are a key component of the colonic cell membrane. Their levels may thus be expected to decrease when tissue is inflamed and thus damaged.

3. Using multivariate analysis, the intensities of these five peaks (the three carotenoid and the two phospholipid) were found to be statistically significantly different between the Raman spectra of the endoscopic MH and the endoscopically inflamed tissue. A similar result was obtained for the histologically assessed samples with four of the same five peaks (three carotenoid and one phospholipid) also significantly different between the spectra of the histologically healed and the histologically active tissue.

This study shows that Raman spectroscopy can be used to discriminate between quiescent and inflamed colon tissue, as assessed either endoscopically or histologically, and thus illustrates its potential as a diagnostic tool for the evaluation of MH in patients with UC. Possible applications of Raman spectroscopy could thus be as an in-vivo adjunct during endoscopy or for rapid assessment of tissue samples taken in endoscopy units. Larger studies to look at whether using these spectral biomarkers can help predict patients at risk for adverse outcomes like relapse of disease activity or lack of response to medical therapy are required.

Acknowledgements